compounds were found to be soluble in benzene which is a further indication of their stability toward disproportionation since MgCl·2THF and $Mg(BH_4)_2$·4THF are not soluble in benzene. X-ray powder-pattern data (Table IV) also indicate the absence of a physical mixture of MgX_2 and $Mg(BH_4)_2$ since no lines characteristic of MgX_2·*n*THF were found. Ebullioscopic molecular weight studies in refluxing tetrahydrofuran showed both $ClMgBH_4$ and $BrMgBH_4$ to be monomeric.

Reactions of HMgX compounds in THF with olefins, alkynes, ketones, etc., are in progress.

Acknowledgment. The financial support by the Office of Naval Research Contract No. N00014-67-A-0419-005AD and contract authority No. 093-050/7-11-69(473) is gratefully acknowledged.

Registry No. HMgCl, 63866-76-2; HMgBr, 63866-75-1; $MgCl_2$, 7786-30-3; $MgBr_2$, 7789-48-2; MgH_2, 7693-27-8; AlH_3, 7784-21-6; B_2H_6, 19287-45-7; $ClMgAlH_4$, 63937-04-2; $BrMgAlH_4$, 63937-03-1; $ClMgBH_4$, 12227-98-4; $BrMgBH_4$, 63866-77-3; DMgCl, 63866-78-4; DMgBr, 63866-79-5.

References and Notes

(1) To whom all inquiries should be addressed.
(2) R. A. Firestone, *Tetrahedron Lett.*, 2029 (1967).
(3) E. Wiberg and P. Strebel, *Justus Liebigs Ann. Chem.*, **607**, 9 (1957); P. Strebel, Dissertation, University of Munich, Oct 1958.
(4) W. E. Becker and E. C. Ashby, *Inorg. Chem.*, **4**, 1816 (1965).
(5) T. N. Dymova and N. G. Eliseeva, *Russ. J. Inorg. Chem.* (*Engl. Transl.*), **8**, 820 (1963).
(6) W. E. Becker and E. C. Ashby, *J. Org. Chem.*, **29**, 954 (1964).
(7) M. J. Rice, Jr., and P. J. Andrellos, Technical Report to the Office of Naval Research, Contract ONR-494(04), 1956.
(8) E. C. Ashby, R. A. Kovar, and K. Kawakami, *Inorg. Chem.*, **9**, 317 (1970).
(9) T. L. Brown, D. W. Dikerhoof, D. A. Bafus, and G. L. Morgan, *Rev. Sci. Instrum.*, **33**, 491 (1962).
(10) E. C. Ashby, R. D. Schwartz, and B. D. James, *Inorg. Chem.*, **9**, 325 (1970).
(11) H. C. Brown and N. M. Yoon, *J. Am. Chem. Soc.*, **88**, 1466 (1966).
(12) E. C. Ashby and R. C. Arnott, *J. Organomet. Chem.*, **14**, 1 (1968).
(13) N. A. Bell and G. E. Coates, *J. Chem. Soc.*, 692 (1965); G. E. Coates, and P. D. Roberts, *J. Chem. Soc. A*, 1008 (1969).
(14) E. C. Ashby, P. Claudy, and R. D. Schwartz, *Inorg. Chem.*, **13**, 192 (1974).

Contribution from the Department of Chemistry, University of Maryland, College Park, Maryland 20742

Theoretical Studies of Valence Orbital Binding Energies in Solid ZnS, ZnO, and ZnF_2

J. A. TOSSELL

Received May 6, 1977 AIC70330H

SCF-Xα scattered wave MO cluster calculations are presented for the ZnS_4^{6-}, ZnS_6^{10-}, ZnO_4^{6-}, ZnO_6^{10-}, ZnF_4^{2-}, and ZnF_6^{4-} molecular clusters and for diatomic ZnS. In solid ZnS the Zn 3d levels are essentially core orbitals lying about 7.5 eV below the S 3p nonbonding orbitals. In solid ZnO this energy difference is reduced to about 6 eV and the orbitals at the top of the valence region have significant Zn 3d–O 2p antibonding character. In solid ZnF_2, bonding and antibonding Zn 3d–F 2p orbital sets are clearly evident at the top of the valence region and have an energy separation of about 4 eV. SCF-Xα photoionization transition state calculations for the ZnF_6^{4-} cluster accurately predict both the energy and relative intensity of the peaks in the XPS spectrum of ZnF_2(s). The observed and calculated ligand p–Zn 3d energy differences in these solids are smaller than those calculated and observed for gas-phase molecules of the same stoichiometry by 2–4 eV. This difference can be understood qualitatively in terms of the ionic model.

I. Introduction

Zn^{2+} is four-coordinate in the binary compounds ZnS(s) and ZnO(s) but six-coordinate in ZnF_2(s). Zn^{2+} also exists in six-coordination with oxygen in $ZnCO_3$(s) and a number of other oxidic compounds, while it is six-coordinate with S only in the high-pressure compound ZnS_2(s).[1]

Based on considerations of ionic radius ratio[2] and the similarity in ionic radius of Zn^{2+} and Mg^{2+},[3] zinc would be expected to prefer six-coordination with oxygen as does Mg^{2+}. The preference of Zn^{2+} for four-coordination has often been explained in terms of its high electronegativity and consequent strong capacity for covalent bonding.[4] A scheme for predicting fractional ionicity from dielectric constant data[5-7] has correctly predicted the four-coordination of Zn^{2+} in ZnO. A similar method based on orbital binding energy differences in x-ray photoelectron spectra (XPS) has found ZnO to be in the ionicity range expected for four-coordination.[8]

However, our recent theoretical study of the electronic structure of ZnO[9] resulted in a new assignment of the ZnO valence region x-ray photoelectron spectrum (XPS) which yielded a spectral ionicity higher than that expected for a four-coordinate material. In addition, valence region XPS studies of ZnF_2[10] showed two widely separated peaks which were attributed to crystal field splitting within the Zn 3d orbitals, a feature not present in the spectrum of ZnO or ZnS.[11] SCF-Xα molecular orbital calculations on Zn^{2+} in tetrahedral and octahedral coordination with oxygen[12] also showed substantial differences in the degree of mixing of Zn 3d and O 2p orbitals as a function of coordination number, as well as in the crystal field splitting within the Zn 3d–O 2p antibonding or crystal field orbitals. These considerations have led to a more complete study of the series of zinc–ligand clusters ZnO_4^{6-}, ZnO_6^{10-}, ZnS_4^{6-}, ZnS_6^{10-}, ZnF_6^{4-}, and ZnF_4^{2-} using the SCF-Xα scattered wave cluster MO method.[12] The calculational methods and results are described in sections II and III and compared with available experimental data in section IV. In section V we compare the electronic structures of Zn-containing gas-phase molecules and solids of the same stoichiometry and of four- and six-coordinate solid polymorphs. Section VI considers methods for the prediction of Zn coordination number.

II. Calculational Method

The SCF-Xα method has been thoroughly reviewed.[13] It is a computationally efficient, first principles, molecular orbital cluster technique which employs Slater's statistical exchange approximation and a multiple scattering technique similar to that of the KKR method of band theory. The MO energies obtained by this technique correspond well to the density of states maxima observed in the XPS of many metal oxides (e.g., MgO, Al_2O_3, TiO_2).[14] Band widths, on the other hand, are observed experimentally to be larger than the spread of cluster MO energies, as might be expected. The SCF-Xα method also gives accurate energies and intensities for optical transitions[15] if the cluster involved is isolated from its surroundings, as is $FeCl_4^-$ in salts with, e.g., tetramethylammonium as counterion. In homodesic crystals, the SCF-Xα cluster approach sometimes yields accurate optical transition energies[16] and sometimes does not.[17] The accuracy of the result

Table I

	α		R(S)[a]			R-
	M	L	M	L	OUT[b]	(M-L)[b]
ZnS_4^{6-}	0.7167	0.72475	1.39	1.48	3.82	2.34
ZnS_6^{10-}			1.39	1.50	3.98	2.48
ZnO_4^{6-}		0.7445	1.32	1.04	3.02	1.98
ZnO_6^{10-}			1.33	1.03	3.16	2.13
ZnF_4^{2-}		0.7373	1.26	1.01	2.89	1.88
ZnF_6^{4-}			1.36	1.09	3.12	2.03

[a] Distances in A. [b] All distances typical of those in solids, except for the hypothetical ZnF_4^{2-} cluster for which R(Zn-F) was chosen 0.15 A shorter than that observed for octahedrally coordinated ZnF_2.

seems to be dependent on the magnitude of curvature of the energy vs. wave vector plot in the conduction band of the material and on the extent to which the optical excitation is localized.

A great advantage of this method for the present study lies in the applicability of a "transition-state"[13] approach to the calculation of orbital binding energies. By performing the SCF-Xα calculation for an electronic configuration with one-half an electron removed from the orbital undergoing ionization, we can account for the electronic relaxation which occurs during ionization which is often substantial (e.g., ref 10 and 11, see also ref 18). It is essentially impossible to take account of this effect using band theory, since the photoelecton hole and the attendant relaxation must be treated as being localized. For this reason comparison of the observed binding energies of tightly bound orbitals with band theory orbital energies is somewhat suspect, as we show in more detail later.

In the SCF-Xα method we require the selection of statistical exchange parameters, α, which are well defined,[19] and sphere radii, R(S), which are somewhat ambiguous. The best results[20] are usually obtained if the ratio of the R(S) are chosen such that before the initiation of the self-consistency process the atomic spheres contain a number of electrons equal to their atomic number and if the absolute values of R(S) are chosen so that the spheres overlap by 10–20%. α, R(S), and R(M–L) values used in this work are given in Table I. The Zn–L distances chosen are typical values for the particular type of bond in a solid. Zn–L distances are therefore chosen about 0.15 Å longer in the octahedral than in the tetrahedral clusters.

III. Results of Calculations

SCF-Xα MO diagrams for the tetrahedral and octahedral Zn^{2+}–ligand clusters ZnS_4^{6-}, ZnS_6^{10-}, ZnO_4^{6-}, ZnS_6^{10-}, ZnF_4^{2-}, and ZnF_6^{4-} are given in Figures 1–3. In each figure the L (ligand) nonbonding orbitals ($1t_1$ in tetrahedral and $1t_{1g}$, $1t_{2u}$, $3t_{1u}$ in octahedral symmetry) are taken as the relative zero of energy. This is for purposes of comparison between the tetrahedral and octahedral clusters only; the binding energies of S 3p, O 2p, and F 2p nonbonding orbitals are of course substantially different, as will be considered later. Although core orbital energies are not shown, the core electrons were included in the SCF process and their energies were determined.

The clusters all show a similar sequence of orbital energies, which we describe fully only for ZnS_4^{6-}. The $1a_1$ and $1t_2$ orbitals are basically ligand 3s orbitals, with little Zn admixture. Next in ground state orbital energy are the 1e and $2t_2$ orbitals, which are predominantly Zn 3d. Above these lie the $1a_1$ and $3t_2$ which are Zn–S 3p bonding orbitals and at the top of the valence orbital set are the 2e, $4t_2$, and $1t_1$ orbitals. The $1t_1$ is pure ligand p, while the 2e and $4t_2$ are either ligand p nonbonding or weakly antibonding, depending upon the particular cluster considered. The lowest energy empty orbitals are the antibonding $3a_1$ and $5t_2$. Orbital sets with similar character occur in the octahedral clusters.

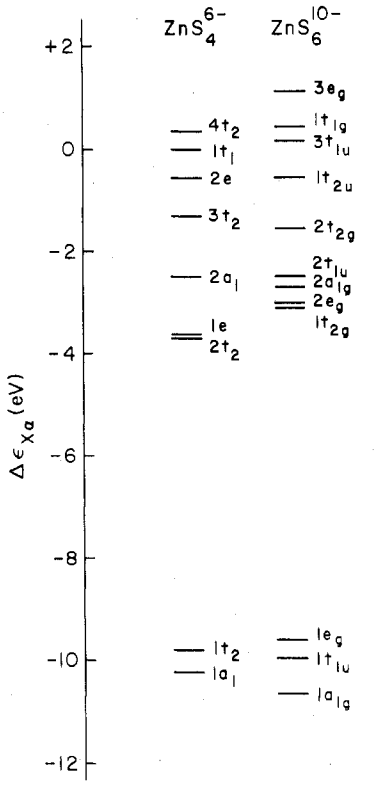

Figure 1. SCF-Xα MO diagrams for ZnS_4^{6-} and ZnS_6^{10-} (relative energies in eV, with respect to $1t_1$ in tetrahedral and average of $1t_{1g}$, $3t_{1u}$, $1t_{2u}$ in octahedral symmetry).

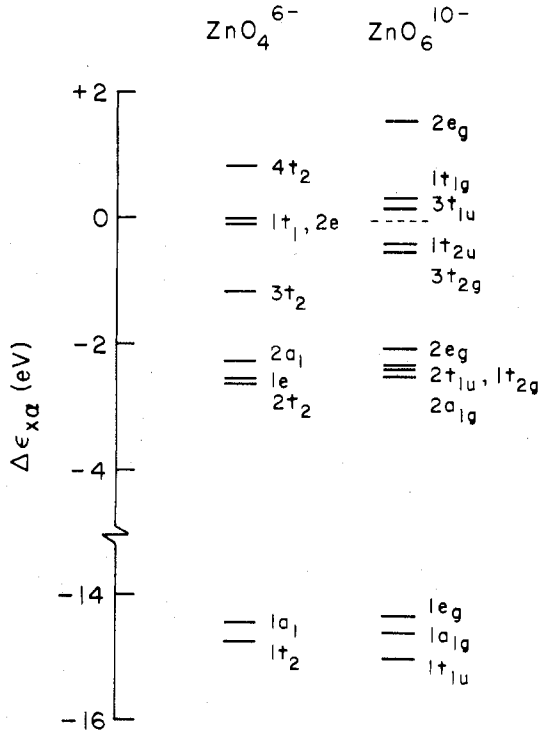

Figure 2. MO diagrams for ZnO_4^{6-} and ZnO_6^{10-}.

In comparing the sulfide, oxide and fluoride clusters for a given coordination number we first observe a change in the separation of the ligand p nonbonding orbitals and the ligand s orbitals from 10 eV for the sulfide to 14–15 for the oxide to 18–19 for the fluoride. The separation of the 1e, $2t_2$ Zn 3d type orbitals from the ligand p nonbonding decreases slightly from sulfide to oxide to fluoride (from about 4 to 2

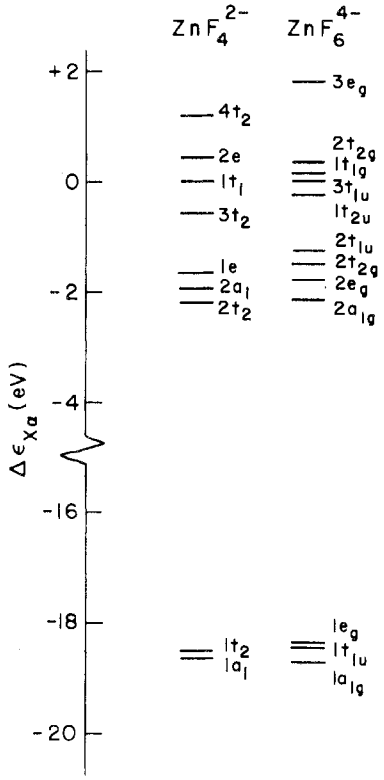

Figure 3. MO diagrams for ZnF_4^{2-} and ZnF_6^{4-}.

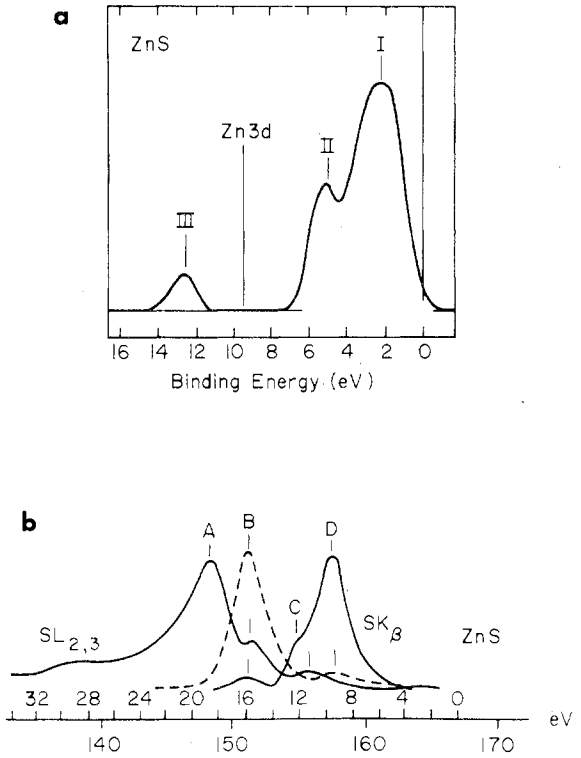

Figure 4. (a) XPS spectrum of ZnS (from ref 11, high-intensity Zn 3d peak replaced by spike); (b) XES spectra of ZnS (from ref 22).

eV) as does the separation of the $2a_1$ Zn 3s–L p bonding orbital and the ligand p (from 2.5 to 2.0 eV). The amount of destabilization of the 2e and $4t_2$ antibonding orbitals, with respect to the $1t_1$ orbital, increases by about 1 eV along the series from sulfide to fluoride.

The change in ligand p–ligand s energy difference is of course consistent with atomic trends. The reduced $2a_1$ orbital stability in the fluoride is consistent with the expected lower degree of covalency in the fluoride, although the difference is small. The variations in the 1e, $2t_2$ and 2e, $4t_2$ orbital energies are more interesting and that for the 2e, $4t_2$ is rather unexpected. They will be considered in more detail in the next section of the paper in which we present not ground state but photoionization transition state energies for these orbitals and compare them with the photoelectron spectra.

In comparing the tetrahedral and octahedral clusters, we note that the $2a_1$ in the tetrahedral cluster and $2a_{1g}$ in the octahedral have very similar energies for all three ligands. This suggests that the extent of Zn 4s covalency is in all cases quite small, in contradistinction to other metal–ligand polyhedra such as those of C and O or Si and O in which such orbitals are highly stabilized by the reduced M–L distance associated with a reduction of coordination number.[21] Between tetrahedral and octahedral coordination there are, however, significant changes in the ground state orbital energies of the 1e, $2t_2$, 2e, and $4t_2$ orbitals and their octahedral equivalents. For these orbitals, however, photoionization transition state eigenvalues are more relevant than those of the ground state and we thus defer our discussion of them.

IV. Orbital Binding Energies in ZnS(s), ZnO(s), and ZnF_2(s) from X-Ray Spectra and MO Calculations

ZnS and ZnO. The electronic structure of II–VI semiconductors, such as ZnO and ZnS, is of considerable general interest in solid state science and has prompted many experimental and theoretical studies. The x-ray photoelectron[11] and x-ray emission[22,23] spectra of ZnS have been well studied. The assignment of the x-ray spectra is analogous to that given for ZnO in ref 9. The spectra of ZnS(s) are shown in Figure 4.

Table II. Comparison of Energies of Peaks in XPS of ZnS(s) with Ground State and Photoionization Transition State Orbital Energies of ZnS_4^{6-} (Energies in eV)

Peak[a]	Assignment	Exptl ΔE[b]	Rel orbital energies ground state	SCF-Xα transition state
I	$4t_2$, $1t_1$, 2e	0	0	0
II	$3t_2$, $2a_1$	−3.0	−1.3, −2.5	−1.3, −2.5
Zn 3d	1e, $2t_2$	−7.3	−3.6, −3.7	−7.6, −7.7
III	$1a_1$, $1t_2$	−10.3	−9.8, −10.2	−9.8, −10.2

[a] Terminology from ref 11. [b] Reference 11, Figure 11.

In the XPS spectrum, the two peaks at binding energies of about 2 and 5 eV are assigned to the $4t_2$, $1t_1$, 2e S 3p nonbonding orbital set and to the $3t_2$, $2a_1$ bonding orbital set, respectively, while the feature at 13 eV is assigned to the S 3s orbitals, $1a_1$ and $1t_2$. The XPS binding energies for these orbital sets are in good agreement with their relative ground state orbital energies, as is shown in Table II. The Zn 3d peak at 9 eV, however, is in clear disagreement with the calculated ground state energies of the 1e and $2t_2$ (predominantly Zn 3d) orbitals. This discrepancy is removed if we performed the appropriate photoionization transition state calculation for the ZnS_4^{6-} cluster. The transition state orbital energies for the 1e and $2t_2$ orbitals are found to be almost 8 eV larger than that of the $1t_1$, an increase in relative stability of about 4 eV from the ground state result. On the other hand, for all orbitals other than 1e, $2t_2$, 2e, and $4t_2$, the relative transition state and ground state orbital energies are found to be equal to within a few tenths of an electron volt. Thus, the transition state binding energies for all the orbital sets are in quite good agreement with the peaks in the valence regions XPS, as shown in Table II.

Given the large electronic relaxation apparent in the SCF-Xα results it would seem to be a dubious procedure to evaluate the accuracy of band theory calculations on Zn

compounds by directly matching Zn 3d orbital energies to the photoelectron spectra, as is the common practice.[24] A comparison of ground state orbital energies and photoelectron spectra energies will, however, be appropriate for those orbitals which are predominantly ligand in character. Ley et al.[11] found that several band structure calculations for ZnS gave results for predominantly sulfur orbitals in good agreement with the XPS spectrum, the quality of the agreement being similar to that shown in Table II for the SCF-Xα results. However, for the separation of the S 3p nonbonding and Zn 3d orbitals none of the band calculations[25] give results as accurate as that of the SCF-Xα calculations. Part of the discrepancy may be a result of the neglect of relaxation effects.

The x-ray emission spectra[22] of ZnS shown in Figure 4b may easily be assigned using the above interpretation of the XPS in conjunction with the electric dipole selection rules for x-ray emission. The main peak, D, in the SK_β XES arises from the S 3p nonbonding orbital set and peak C from the Zn–S bonding orbital set. Peak B, which appears in both XES and XPS, arises from the Zn 3d orbitals while peak A, most prominent in the $SL_{2,3}$ spectrum, is assigned to the S 3s orbitals. A shoulder in the $SL_{2,3}$ spectrum, coincident with peak B in XPS, indicates some mixing of S 3s character into the Zn 3d orbital. Peak separations in XES are virtually identical to those observed in the XPS.

It is thus clear that ZnS has an upper valence region consisting of a S 3p nonbonding and a Zn–S bonding orbital set, which are separated by about 3 eV. The Zn 3d orbitals lie about 7–8 eV below the S 3p nonbonding orbitals and are essentially nonbonding. In the latter respect ZnS differs decisively from the d^{10} sulfide Cu_2S, in which the 3d orbitals are about 3 eV less tightly bound than the S 3p.[22] The difference in relative 3d orbital energies between these two compounds is about 8 eV (taking the difference of S 3p nonbonding orbital binding energies into account). From comparison of ground state orbital energy diagrams it appears that about half of this difference arises from the greater electronic relaxation within the 3d shell attendant upon ion formation in ZnS.

Note that the position of the Zn 3d levels in ZnS(s) was until recently in considerable dispute.[25] Neither optical absorption data nor band calculations could convincingly determine its binding energy. Application of periodic table systematics was also unsuccessful, primarily because the variation in electronic structure at the end of the first transition series does not follow the systematic trend observed in earlier parts of the series.[9,25,26]

The electronic structure of ZnO is very similar to that of ZnS; XPS and XES features show a one-to-one qualitative correspondence, although there are of course quantitative differences. The separation of S 3p nonbonding and Z–S 3p bonding orbital peaks is about 0.2 eV less and that of S 3p nonbonding and Zn 3d about 1.3 eV less. The x-ray spectra of ZnO have been previously discussed using SCF-Xα cluster model results.[9] Note that although the 2e and $4t_2$ orbitals of the ground state of ZnO_4^{6-} are mostly S 3p in character they do have about 40–45% of their electron density either in the Zn sphere or in the interatomic region; thus they should be described as weakly antibonding Zn 3d–O 2p orbitals. Even in the transition states appropriate to x-ray emission these orbitals have a few percent Zn 3d character, consistent with the appearance of weak features at high energies in the ZnL XES of ZnO.[26] Thus the top of the valence region in ZnO does possess some Zn 3d character, consistent with the high catalytic activity of this material.

ZnF_2. For the solid compound ZnF_2, considerably less experimental spectral data are available; what are available are much different from those of ZnS and ZnO. The valence region XPS spectrum of ZnF_2(s) from ref 10, Figure 4, is shown in Figure 5. Based on their observed energy for the F 2s peak (not shown in Figure 5) and the F 2p–F 2s separation they observed in other fluorides, Kowalczyk et al. estimated the F 2p peak, of low intensity, to fall at the position shown. The remainder of the XPS could be analyzed into an intense peak at 12 eV and a less intense but still distinct peak at about 8 eV. Kowalczyk et al. give sound arguments based on relative Zn 3d/F 2p intensities and average Zn 3d energies for assigning both features to Zn 3d type orbitals. Contrary to their interpretation, however, the splitting of the 12 and 8 eV peaks is *not* a crystal field t_{2g}–e_g splitting but is rather a separation of the bonding ($1t_{2g}$, $2e_g$) and antibonding ($2t_{2g}$, $3e_g$) Zn 3d–F 2p orbital sets. Using this interpretation, calculated photoionization state transition energies for ZnF_6^{4-} are in good agreement with experiment, as is shown in Table III. We have also estimated the relative intensities of these two peaks from the SCF-Xα results by totaling the amount of Zn 3d character in the various Zn 3d–F 2p orbitals, using the spatial electron density distributions calculated for the photoionization transition states. The total number of d electrons within the Zn sphere is 8.86 for the $1t_{2g}$ and $2e_g$ bonding orbitals and 2.44 for the $2t_{2g}$, $3e_g$ antibonding orbitals. The ratio of number of d electrons is thus 3.6, very similar to the intensity ratio of 3.5:1 observed in ref 11. (Note that the large Zn sphere radius causes the total number of d electrons to be greater than 10.)

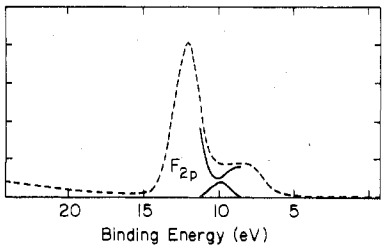

Figure 5. XPS of ZnF_2(s) (from ref 10).

Table III. Comparison of Experimental and Calculated XPS Peak Maxima Separations in ZnF_2(s) (Energies in eV)

Orbital assignment of peak	Exptl	Calcd
Zn 3d–F 2p antibonding ($3e_g$, $2t_2$)	0	0
F 2p nonbonding	−1.7[a]	−0.3
Zn 3d–F 2p bonding ($1t_{2g}$, $2e_g$)	−3.9	−4.3
F 2s	−20.9	−18.8

[a] Estimated on the basis of F 2p–F 2s separation of 20.9 eV in fluorides.

The observed difference between ZnS(s) and ZnF_2(s) is probably a result of two factors. First, the F 2p orbitals are more tightly bound than the S 3p and thus closer in energy to the Zn 3d. Second, the Zn 3d orbitals are less stable in the six-coordinate cluster ZnF_6^{4-}, occurring in ZnF_2(s), than they are in the (hypothetical) ZnF_4^{2-} cluster; thus the difference in coordination number between ZnS(s) and ZnF_2(s) may have some effect.

From the point of view of Zn 3d–Lp mixing, the ZnF_6^{4-} cluster is the most covalent of those described in this paper. The antibonding orbitals $2t_{2g}$ and $3e_g$ have more Zn 3d character (19–28%) and the bonding orbitals $1t_{2g}$ and $2e_g$ more F 2p character (9–15%) than for any of the other clusters. The enhanced covalency in the fluoride is presumably a result not of increased orbital overlap but of a reduction in Zn 3d–L p energy difference.

V. Variations in Electronic Structure between Gaseous Diatomic, Four-Coordinate Solids and Six-Coordinate Solid Zn Compounds of Given Stoichiometry

The electronic structure of ZnF_2(s) is surprising in two

Table IV. Zn 3d Bonding and Antibonding Photoionization Transition State Orbital Energies in Various Clusters[a]

	ZnS_4^{6-}	ZnS_6^{10-}	ZnO_4^{6-}	ZnO_6^{10-}	ZnF_4^{2-}	ZnF_6^{4-}
Antibonding (2e, $4t_2$ or $2t_{2g}$, $3e_g$)	−0.04	−0.59	+0.42	−0.07	+0.47	+0.33
Bonding[b] (1e, $2t_2$ or $1e_g$, $2t_{2g}$)	−7.67	−7.83	−5.84	−5.19	−4.88	−4.00
Av of bonding and antibonding orbital energies	−3.86	−4.21	−2.75	−1.63	−2.20	−1.83
2e-$4t_2$ or $2t_{2g}$-$3e_g$ splitting	0.86	2.62	0.90	2.08	0.81	1.52

[a] In eV, with respect to $1t_1$ energy in tetrahedral and $1t_{1g}$, $1t_{2u}$, $3t_{1u}$ average energy in octahedral clusters. [b] Essentially Zn 3d core in ZnS, ZnO.

respects. First, it differs greatly from that of ZnS(s) and ZnO(s), in which the Zn 3d orbitals are quite corelike and Zn 3d character at the top of the valence region is small. Second, it differs in much the same way from the electronic structures of $ZnCl_2$(g) and presumably ZnF_2(g). The UV photoelectron spectra[27,28] or ZnI_2(g), $ZnBr_2$(g), and $ZnCl_2$(g) show the Zn 3d orbitals to be corelike and to be well separated from the top of the valence region. This separation is about 7.2 eV in $ZnCl_2$ and based on trends[27,28] within the Zn dihalide series the corresponding separation in ZnF_2 would probably be about 6.5. Thus in ZnF_2(g) we would expect very little Zn 3d–F 2p interaction. This expectation is supported by ab initio Hartree–Fock calculations[29] on ZnF_2(g) which show essentially no mixing of Zn 3d and F 2p orbitals and give a Zn 3d–F 2p ground state orbital energy separation of 8.4 eV. This value is in reasonable agreement with (extrapolated) experiment, particularly considering the neglect of relaxation effects, which should be larger for the Zn 3d orbitals and which would tend to decrease their relative ionization potentials. (Note that the Hartree–Fock and the SCF-Xα methods define orbital energies differently, so that relaxation corrections in the two methods are apparently opposite in direction.)

This difference between the electronic structures of gaseous molecules and the corresponding solids is also observed for ZnS. An ab initio SCF calculation[30] on diatomic ZnS(g) found the separation of Zn 3d and S 3p nonbonding orbitals to be about 15 eV, compared to about 7 eV observed in the solid. Although part of this difference may arise from the failure of Koopmans' theorem it seems probable that there is a real difference of M 3d–L 2p energies between gas and solid. Our preliminary SCF-Xα calculations on diatomic ZnS with the same Zn–S distance observed in ZnS(s) give a difference in photoionization transition state energies of about 10.8 eV between the highest occupied orbital (3π, >80% S 3p in character) and the Zn 3d orbitals, with a splitting within the Zn 3d orbital set of about 0.05 eV. As in the Hartree–Fock calculation, the Zn 3d orbitals are found to be even more tightly bound than the S 3s (by a few tenths of an electron volt). In diatomic CuO(g) preliminary SCF-Xα calculations[31] show the Cu 3d orbitals to be more tightly bound than the O 2p nonbonding orbitals by about 2 eV, while in CuO(s) both SCF-Xα calculations[9] and experiment[26] show Cu 3d–O 2p difference to be about 2 eV in the opposite direction. Thus it is clear that the electronic structures of diatomic transition metal containing molecules may, and generally will, differ greatly from those of the corresponding solids.

This difference between gas and solid state results can be understood qualitatively using an ionic model, at least for the case of ZnF_2 and ZnS. Using values of 39.7 eV for the third IP of Zn[32] and 3.45 eV for the electron affinity of F[33] and calculating the Madelung potential for fully charged ions with R(Zn–F) = 1.81 Å[34] and a linear structure, we obtain a Zn 3d–F 2p energy difference of 8.4 eV in ZnF_2(g) while a similar approach for ZnF_2(s) (with R(Zn–F) = 2.03 Å, using the method applied by Poole et al. [35]) gives an energy difference of about 2.3 eV. Thus the major part of the difference in electronic structure of ZnF_2(g) and ZnF_2(s) is a result of the difference in the magnitude of the Madelung term. This difference arises from the higher coordination number in the solid, overwhelming the increase in nearest neighbor distance which would tend to reduce the term. With a small Zn 3d–F 2p energy separation in the ionic limit, we would expect increased covalent mixing to give rise to bonding and antibonding Zn 3d–F 2p orbital sets. Using −4.0 eV for the affinity of S for two electrons[36] we obtain S 3p–Zn 3d separations of about 19 and 3 eV for diatomic and solid ZnS, respectively. Although the trend is in the right direction, the difference is considerably larger than that obtained from the SCF-Xα calculations.

It is also of some interest to compare the Zn 3d orbital energies found in the tetrahedral and octahedral clusters. This comparison is given in Table IV. We find that the splitting of the t_{2g} and e_g antibonding orbitals is larger in octahedral coordination than in tetrahedral by a factor of 2–3, consistent with the ratio of 9/4 predicted from the simplest possible crystal field approach.

The Zn 3d orbitals are considerably more stable with respect to the ligand p nonbonding orbitals in the sulfide than in the oxide or fluoride. This is not a result of changes in the absolute binding energies of the Zn 3d levels, which are virtually identical at least in ZnS and ZnO.[11,37] The difference is rather a result of variation in the L p binding energies, estimated as 4, 7, and 8 eV for sulfides, oxides, and fluorides, respectively.[38] For the sulfide both the Zn 3d–L p bonding orbital energies and the average Zn 3d orbital energy are lowered in going from four- to six-coordination. For the fluoride the opposite effect occurs. Thus the changes in Zn 3d energies are in a direction opposite to that needed to stabilize four-coordinate Zn^{2+} in sulfides and six-coordinate Zn^{2+} in fluorides.

VI. Prediction of the Coordination Number of Zn

Since total energies are so difficult to accurately calculate, most methods for predicting stability focus instead upon changes in one-electron orbital energies. Examples are the Hückel theory of organic chemistry and the crystal field theory of transition metal chemistry.

The XPS based theory of Kowalczyk et al.[8] focuses on the energy separation of peaks II and III in the XPS spectrum (see Figure 4) which correspond to bonding orbitals and anion s nonbonding orbitals for the Zn compounds considered here. The covalent contribution to this energy difference is found to be (in eV) $\Delta E_s^c = 8.0 - 2.2 \times$ (nearest neighbor distance in Å). The difference of the observed splitting and the covalent term is the ionic contribution ΔE_s^i and the fractional ionicity is set equal to $F_i^{XPS} = \Delta E_s^i / \Delta E_s$. Kowalczyk et al. showed that if F_i is greater than 0.67 the material is observed to be six-coordinate while if F_i is lower than 0.67 the compound will be four-coordinate.

For ZnS and ZnO they calculate fractional ionicities of 0.61 and 0.59 consistent with four-coordination. For ZnO, however, our calculations (ref 9 and present work) indicate that peak III (the O 2s peak) is the peak observed at about 21 eV, not that at 15 eV as assumed by Kowalczyk. Using our assignment the O 2p nonbonding orbital–O 2s orbital separation is 18 eV, quite similar to that observed[39] in other four-coordinate oxides, e.g., SiO_2. The calculated fractional ionicity will thus increase to 0.76, which would lead to a prediction of six-coordination in ZnO. Since the Zn 3d peaks overlap

peak type II in ZnF_2, no prediction based on the XPS model can be definitely made, although on the basis of the results for other fluorides one would expect F_i to be substantially larger than 0.67.

An alternative approach is that of Phillips[5] and Van-Vechten.[6] They obtain the average energy gap between valence and conduction bands, E_g, from the static dielectric constant and wet its covalent part $E_h \propto$ (nearest neighbor distance)$^{-2.5}$. The ionic part $C = (E_g^2 - E_h^2)^{1/2}$. For ZnS and ZnO, with dielectric constants of 5.2 and 3.7, respectively (N.B. new value of $\epsilon(0)$ for ZnO, see ref 7), the average band gaps are 7.8 and 12.3 eV, and the calculated fractional ionicities $F_i^{\text{dielectric}} = C^2/E_g^2$ are 0.62 and 0.65. These ionicity values fall below the cutoff value of 0.785 for the transition from four- to six-coordination found by Phillips. Besides correctly predicting coordination number in ZnS and ZnO the Phillips scale can also qualitatively predict the enthalpy difference between the four- and six-coordinate polymorphs of ZnS and ZnO.[7]

The large difference between the average band gaps of ZnS and ZnO cannot be attributed to larger orbital energy separations within the valence orbitals of ZnO. The separation of L p nonbonding and bonding orbital sets is virtually identical in the two compounds and the Zn 3d levels are only 1.5–2.0 eV lower in the oxide (with respect to the L p nonbonding orbital set). The L s nonbonding orbitals do, however, lie about 8 eV lower with respect to the L p nonbonding orbitals in ZnO than in ZnS.

The UV reflectance spectra of crystalline ZnO and ZnS show their lowest energy electronic transitions at 3.3 and 3.6 eV, respectively. The $4t_2 \rightarrow 3a_1$ optical transition state energy differences from our SCF-Xα calculations are 5.0 and 4.3 eV, respectively. These energies reflect the separation of the top of the valence band and the lowest density of states maximum in the conduction band. Most of the features in the reflectance spectrum of ZnS can be reasonably interpreted using the best available band calculations,[25] although some parameterization is necessary. Since the band gap in ZnO is 3.3 eV, and the O 2p–O 2s separation about 18 eV, the O 2s $\rightarrow$ conduction band excitation energy would be >21 eV, consistent with the observation[40] that the effective number of valence electrons calculated from the UV reflectance spectrum measured up to 22 eV was considerably less than 8 for ZnO. Studies to higher energies should disclose O 2s $\rightarrow$ conduction band transitions. However, the spectrum of ZnO presents additional problems; the intensity of reflection at low energy is much smaller than that obtained from recent band theoretical calculations,[41] even though the calculation used a pseudopotential approach which ignored the Zn 3d electrons. Thus it appears that more accurate band calculations and further study of the UV spectra will be necessary to explain the results. The SCF-Xα results can contribute little in this regard, first because the nature of the empty orbitals will depend upon the cluster boundary conditions and, more importantly, because they can yield at best the maxima of the density of states and cannot describe the curvature of the energy bands as a function of wave vector.

VII. Conclusions

The SCF-Xα method gives MO energies which correspond reasonably well to maxima in the density of states for ZnS(s), ZnO(s), and ZnF_2(s). The use of the transition state procedure is found to be necessary to obtain accurate energy differences between L p and Zn 3d energies. The degree of mixing of Zn 3d and L p orbitals is greatest in the fluoride and is in general larger in the octahedrally coordinated clusters. L p–Zn 3d energy differences are 2–4 eV smaller in Zn containing solids than in the corresponding diatomic molecules, leading to greater Zn 3d–L p mixing in the solid. The stability of Zn in tetrahedral coordination with S and O cannot be explained simply in terms of variations of the one-electron energies of either the Zn–L p bonding orbitals or the Zn 3d orbitals from tetrahedral to octahedral coordination.

Acknowledgment. Acknowledgment is made to the donors of the Petroleum Research Fund, administered by the American Chemical Society, for partial support of this research and to the Computer Science Center of the University of Maryland. The ZnF_2 calculations were suggested to the author by R. G. Burns, and K. H. Johnson pointed out the importance of the Zn 3d character at the top of the valence region in ZnO.

Registry No. ZnS, 1314-98-3; ZnO, 1314-13-2; ZnF_2, 7783-49-5; ZnS_4^{6-}, 63915-41-3; ZnS_6^{10-}, 63915-40-2; ZnO_4^{6-}, 63915-39-9; ZnO_6^{10-}, 63915-38-8; ZnF_4^{2-}, 25862-73-1; ZnF_6^{4-}, 63915-43-5.

References and Notes

(1) A. F. Wells, "Structural Inorganic Chemistry", Claredon Press, Oxford, United Kingdom, 1975.
(2) L. Pauling, *J. Am. Chem. Soc.*, **51**, 1010 (1929).
(3) R. D. Shannon and C. T. Prewitt, *Acta. Crystallogr., Sect.* B, **25**, 925 (1969).
(4) W. S. Fyfe, "Geochemistry of Solids: An Introduction", McGraw-Hill, New York, N.Y., 1964.
(5) J. C. Phillips, *Rev. Mod. Phys.*, **42**, 317 (1970).
(6) J. A. VanVechten, *Phys. Rev.*, **182**, 891 (1969).
(7) A. Navrotsky and J. C. Phillips, *Phys. Rev. B*, **11**, 1583 (1975).
(8) S. P. Kowalczyk, L. Ley, F. R. McFeely, and D. A. Shirley, *J. Chem. Phys.*, **61**, 2850 (1974).
(9) J. A. Tossell, *Chem. Phys.*, **15**, 303 (1976).
(10) S. P. Kowalczyk, L. Ley, F. R. McFeely, R. A. Pollak, and D. A. Shirley, *Phys. Rev. B*, **9**, 381 (1974).
(11) L. Ley, R. A. Pollak, F. R. McFeely, S. P. Kowalczyk, and D. A. Shirley, *Phys. Rev. B*, **9**, 600 (1974).
(12) J. A. Tossell, Geological Society of American Annual Meeting, Denver, Colo., Sept. 1976.
(13) K. H. Johnson, *Adv. Quantum Chem.*, **7**, 143 (1973); J. C. Slater, *ibid.*, **6**, 1 (1972).
(14) S. P. Kowalczyk, F. R. McFeely, L. Ley, V. T. Gritsyna, and D. A. Shirley, *Solid State Commun.*, in press.
(15) L. Noodleman, *J. Chem. Phys.*, **64**, 2342 (1976).
(16) J. A. Tossell, *J. Am. Chem. Soc.*, **97**, 4840 (1975).
(17) J. A. Tossell, *J. Phys. Chem. Solids*, **36**, 1273 (1975).
(18) W. E. Spicer, *Phys. Rev.*, **154**, 385 (1967).
(19) K. Schwartz, *Phys. Rev. B*, **5**, 2466 (1972).
(20) J. G. Norman, Jr., *Mol. Phys.*, **31**, 1191 (1976).
(21) J. A. Tossell, *J. Phys. Chem. Solids*, **37**, 1043 (1976).
(22) E. P. Domashevskaya, V. A. Terekhov, L. N. Marshakova, Ya. A. Ugai, V. I. Nefedov, and N. P. Sergushin, *J. Electron Spectrosc.*, **9**, 261 (1976).
(23) C. Sugiura, Y. Goshi, and I. Suzuki, *Phys. Rev. B*, **10**, 338 (1974).
(24) R. A. Powell, W. E. Spicer, and J. C. McMenamin, *Phys. Rev. Lett.*, **27**, 97 (1971).
(25) D. J. Stuckel, R. N. Euwema, T. C. Collins, F. Herman, and R. L. Kortum, *Phys. Rev.*, **179**, 740 (1969).
(26) I. A. Brytov and E. Z. Kurmayev, *Fiz. Met. Metalloved.*, **32**, 520 (1971).
(27) B. G. Cocksey, J. H. D. Eland, and C. J. Danby, *J. Chem. Soc., Faraday Trans. 2*, **69**, 1558 (1973).
(28) A. F. Orchard and N. V. Richardson, *J. Electron Spectrosc.*, **6**, 61 (1975).
(29) D. R. Yarkony and H. F. Schaefer III, *Chem. Phys. Lett.*, **15**, 514 (1972).
(30) A. Hinchliffe and J. C. Dobson, *Theor. Chim. Acta*, **39**, 211 (1975).
(31) J. A. Tossell, unpublished results.
(32) C. E. Moore, *Natl. Bur. Stand. (U.S.), Circ.*, **No. 467** (1952).
(33) R. S. Berry and C. W. Reiman, *J. Chem. Phys.*, **38**, 1540 (1963).
(34) P. A. Akishin and V. P. Spiridonov, *Sov. Phys.-Crystallogr. (Engl. Transl.)*, **2**, 472 (1957).
(35) R. T. Poole, J. D. Riley, J. G. Jenkin, J. Liesegang, and R. G. G. Leckey, *Phys. Rev. B*, **13**, 2620 (1976).
(36) R. S. Berry, *Chem. Rev.*, **69**, 533 (1969).
(37) C. J. Vesely and D. W. Langer, *Phys. Rev. B*, **4**, 451 (1971).
(38) A. S. Koster and H. Mendel, *J. Phys. Chem. Solids*, **31**, 2511, 2523 (1970).
(39) B. Fischer, R. A. Pollak, T. H. DiStefano, and W. D. Grobman, *Phys. Rev. B*, **15**, 3193 (1977).
(40) R. L. Hengehold, R. J. Aimassy, and F. L. Pedrotti, *Phys. Rev. B*, **1**, 4784 (1973).
(41) S. Bloom and I. Ortenberger, *Phys. Status Solidi B*, **58**, 561 (1973).